Available online at www.sciencedirect.com
ScienceDirect
Physica B 391 (2007) 6–11
PHYSICA B
www.elsevier.com/locate/physb

Influence of GaN polarity and intermediate-temperature buffer layers on strain relaxation and defects

C.X. Peng[a,*], H.M. Weng[a], C.F. Zhu[b], B.J. Ye[a], X.Y. Zhou[a], R.D. Han[a], W.K. Fong[c], C. Surya[c]

[a]Modern Physics Department , University of Science and Technology of China, Hefei 230026, People's Republic of China
[b]Materials Science and Engineering Department, University of Science and Technology of China, Hefei 230026, People's Republic of China
[c]Department of Electronic and Information Engineering, The Hong Kong Polytechnic University, Hong Kong

Received 9 November 2005; received in revised form 16 May 2006; accepted 25 May 2006

Abstract

The dependence of strain relaxation and consequent generation defects on Gallium nitride (GaN) polarity and intermediate-temperature buffer layer (ITBL) has been observed by Raman scattering, photoluminescence (PL) and monoenergetic positron beam techniques. Raman scattering studies have indicated that tensile stress prefers and compress stress is present in N-polar and Ga-polar films, respectively. Furthermore, ITBL relaxes strains in Ga-polar GaN films more effectively than in N-polar GaN films. PL results show that peak shifts due to the effect of polarity and ITBL. Depth resolved defect-sensitive *S* parameter measurements, using monoenergetic positron beam, exhibit larger *S* parameter and shorter positron effective diffusion length in N-polar GaN samples than those in Ga-polar films. When ITBL is added, *S* parameter decreases and effective diffusion length increases in both groups. Hall mobility and carrier concentration measurement manifest a reduction of dislocation line and electrons trap centers such as V_{Ga} or Ga vacancy clusters.

PACS: 78.70.Bj; 68.55.Ln

Keywords: GaN polarity; Strain; Defects

1. Introduction

Gallium nitride (GaN) and its alloys have recently attracted extensive attention because of their importance to fabricate optoelectronic devices in the region of blue to ultraviolet light as well as high-temperature electronics. Due to lack of commercial native substrate, (0 0 0 1) oriented sapphire (α-Al_2O_3) usually acts as the substrate to prepare GaN. Because of significant lattice mismatches between GaN and sapphire substrate (>13%) and different thermal expansion coefficients (25%), GaN films typically exhibit large defects and residual strain [1–3]. To grow high-quality GaN films, it is a common practice to deposit a thin buffer layer between GaN epilayer and substrate at relatively low temperature, and this buffer layer provides high-density nucleation centers. The improvement of film quality by the deposition of a thin GaN or AlN low-temperature buffer layer (LTBL) is well exhibited through X-ray diffraction, photoluminescence (PL) spectra, carrier mobility and concentration for metal organic chemical vapor deposition of GaN [4–6]. To a certain extent the implementation of LTBL in molecular beam epitaxy (MBE) growth process proved beneficial. Later many groups further developed the growth method to add an ITBL layer on the base of LTBL, thus the epilayer electrical and optical performance observably elevate [3,7]. However, the mechanisms by which buffer layer relieves stress, and by which stress relaxation affects defect formation are not well understood. Since GaN has a wurtzite structure having polarity along the *c* axis, two different surface structures exhibit the polarity of GaN;

*Corresponding author.
E-mail address: pengcx@mail.ustc.edu.cn (C.X. Peng).

0921-4526/$ - see front matter © 2007 Elsevier B.V. All rights reserved.
doi:10.1016/j.physb.2006.05.431

these are referred to as (0 0 0 1) Ga face and (0 0 0 $\bar{1}$) N face. Polarity has a great effect on crystal quality, however its mechanism is still unclear behind these phenomena. Raman spectroscopy and positron annihilation are powerful tools to investigate stress and defect in materials.

Raman scattering is a nondestructive and sensitive means, used widely to analyze matter microcosmic specialities in physics and chemistry field, and it can reveal much information such as residual stress, size of crystal grain, components in compounds according to location, number, relative intensity and shape of frequency band in Raman spectra. GaN of hexagonal wurtzite structure belongs to C_{6v} space group, group theory predicts such modes:

$$1A1(TO) + 1A1(LO) + 2B1 + 1E1(TO) + 1E1(LO) + 2E2 \quad (1)$$

two $B1$ modes are inactive and silent in Raman spectra, high-frequency mode of $E2$ can be shifted only by stress [8,9]. Raman scattering is a suitable tool to observe stress relaxation.

In crystal, different stress affects the formation energy of vacancy, and misfit dislocation is introduced during the course of strain relaxation. Positron annihilation spectroscopy (PAS) with slow-positron beam is a powerful and sensitive technique to detect open-volume defects in metals, semiconductors, polymers and nanomaterials [10,11]. When a positron is implanted into the condensed matters, it annihilates with an electron mainly into 511 keV γ quanta. The momentum of positron–electron pair causes a Doppler shift in the energy of annihilation photons. In the material containing defects, a freely diffusing positron can be readily localized or trapped at open-volume defects as a result of missing positive-ion cores at these defects. The trapping will lead to a narrowing of the momentum distribution of positron–electron pair and in annihilation photons, which is reflected in the shift of Doppler broadening spectrum. The change of Doppler broadening spectrum is characterized by S parameter and W parameter. S and W parameters demonstrate the fraction of positron–electron pair with low-momentum and high-momentum, respectively. Higher S value for a particular material suggests more annihilation with low-momentum electrons implying greater positron trapping in defects.

2. Experiment

A series of GaN thin films were deposited by rf-MBE on sapphire (0 0 0 1) wafers [12]. The substrate was first degreased and cleaned by a standard cleaning procedure, then it was outgassed within growth chamber at 850 °C, Nitridation of the sapphire wafer was then carried out inside the growth chamber at 500 °C. Subsequently, a thin GaN buffer layer, of thickness approximately 20 nm, was deposited at 500 °C. For sample B, an additional GaN-ITBL was grown at 690 °C on the top of GaN buffer layer, while no ITBL was used for Sample A. The thickness of the ITBL was chosen to be 800 nm, which was found to be the optimal ITBL thickness for our system. The GaN epitaxial layers, of 1.8 μm thickness, were finally grown on the single and double buffer layer systems at 740 °C, respectively. Samples C and D were fabricated with AlN LTB layer deposited at 690 °C; for sample D, an additional 800 nm GaN ITBL was used. The thickness of all epilayers is same. After characterization and analysis, one knows that samples A and B have N polarity while samples C and D reveal Ga polarity [12]. Carrier mobility and concentration at room temperature were measured by a Bio-Rad HL5500 Hall effect measurement system. The information about all samples is listed in the following Table 1:

Raman scattering spectroscopy was measured in Structure Research Laboratory of the University of Science and Technology of China (USTC). The system is LABRAM-HR (France JY), with Ar^+(514.5 nm) and He–Cd (325 nm) laser, the resolution is better than 0.5 cm^{-1}.

Variable energy positron measurements were performed for samples at room temperature with USTC slow positron beam equipment [13]. Positron derived from $Na^{22}\beta^+$ decay was moderated, transported and focused by magnetic field system. The beam diameter is smaller than 10 mm, and its maximum energy dispersion is 2 eV. Positron beam is injected into samples, and implantation depth was modulated by adjusting minus high voltage. Doppler broadening spectra of annihilation radiation were measured with a high purity Ge detector system (ORTECGEM-1075), which has an energy resolution of 1.2 keV (FWHM) at 514 keV rays for ^{85}Sr. Spectra with a total count number of 5×10^5 were measured for every value of energy E. The defect sensitive line parameter, S parameter is defined as the ratio of the integral of ray counts in central energy region at 511 keV to total counts of spectrum; in the same way, W parameter is the ratio of wing area to total area under the spectrum, and it gives the information about the high-momentum electrons.

3. Results and discussion

Figs. 1 and 2 show the high-frequency mode in Raman spectra. Peaks of samples A, B, C, and D locate at 567.1, 567.1, 570 and 568 cm^{-1}, respectively. Compared with 568 cm^{-1} for GaN free of strain [9], Raman peaks of N-polar samples namely A and B situated at low-energy orientation, while Ga-polar sample C peak lies at 570 cm^{-1}, Ga-polar sample D with ITBL its peak is at 568 cm^{-1}. When compressive stress is put on GaN thin film, Raman peak tends to larger wave number; on the other hand, tensile stress is present, and the peak moves to an opposite direction. So it can be concluded Ga-polar GaN specimens show compressive stress while tensile stress exists in the N-polar GaN. Kozawa and his collaborators [14] reported that Raman frequency shift $\Delta\omega$ (in cm^{-1}) obeys following relation $\Delta\omega = 6.2\sigma$, where σ is biaxial compressive or tensile stress in unit of Gpa. Using this relation, we could

Table 1
Information about samples grown and experimental results

Sample	ITBL (GaN)	Polar	n (cm^{-3})	Mobility (cm^2 V^{-1} s^{-1})	S parameter	L_{eff} (nm)	Residual stress (Gpa)
A	No	N-polar	3.93×10^{17}	82	0.4941 ± 0.0003	25.6 ± 1.2	0.129
B	800 nm	N-polar	4.9×10^{17}	377	0.4921 ± 0.0003	31 ± 1.5	0.129
C	No	Ga-polar	3×10^{17}	280	0.4906 ± 0.0003	37 ± 2.6	0.323
D	800 nm	Ga-polar	2.9×10^{17}	430	0.4878 ± 0.0003	46 ± 3.4	0

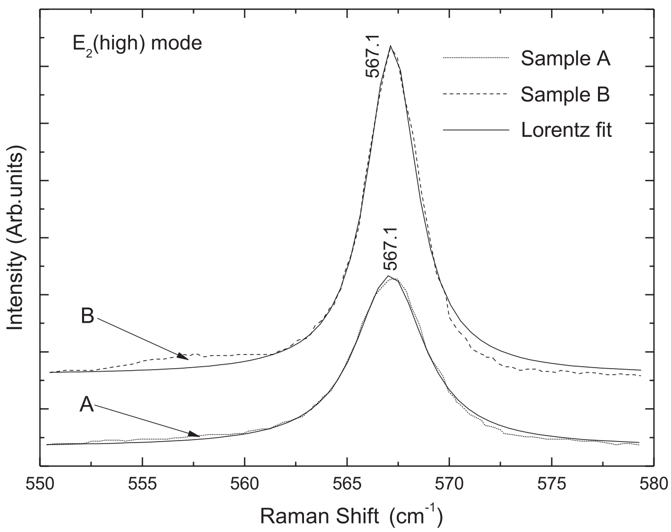

Fig. 1. Raman shifts of E_2 mode showing ITBL effects on N-polarity at room temperature.

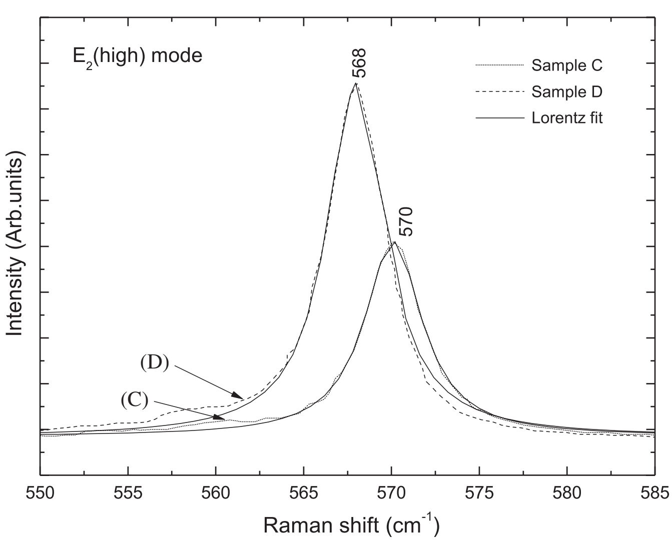

Fig. 2. Raman shifts of E_2 mode showing ITBL effects on Ga-polarity at room temperature.

estimate the residual stress for all samples, the residual stress for samples A, B, C and D is 0.129, 0.129, 0.323 Gpa and nearly zero, respectively. From these values, we can see that ITBL could effectively reduce the residual stress in Ga-polar GaN films, but it does not work well in N-polar films (Fig. 3).

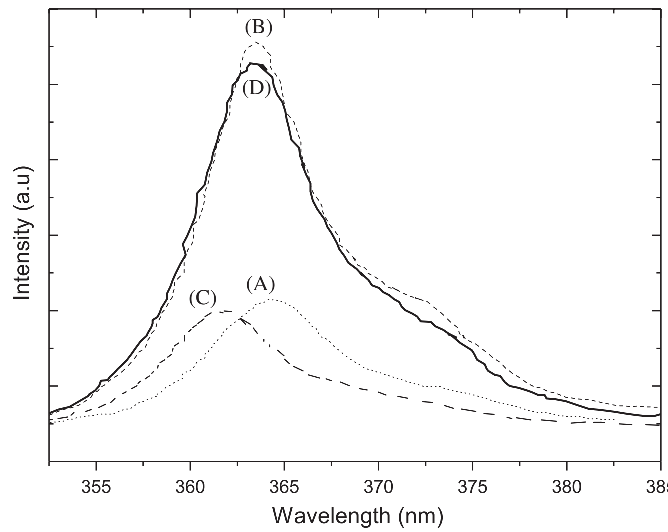

Fig. 3. PL spectra for GaN films at room temperature.

The results of PL spectra exhibit that the PL peaks appear 364.1 nm (3.408 eV), 363.4 nm (3.414 eV), 361.8 nm (3.429 eV) and 363.1 nm (3.417 eV) for A, B, C and D samples at room temperature, respectively [12]. The strain-related phenomena in GaN epitaxial films have been well investigated both experimentally and theoretically [15,16]. A number of authors have shown that relaxation of the residual strain is associated with PL peak shifts [16,17]. These results indicate that band structure of GaN is strongly influenced by residual strain. The excitonic transition energy increases under compressive biaxial strain, and decreases under tensile biaxial strain. Small excitonic transition energy for A and B samples indicates the existence of a large tensile stress in these films, while for C and D samples compressive stress is dominant. Relaxation of residual stress could result in a shift in the excitonic transition energy of material. In contrast to increasing 6 meV excitonic transition energy for N-polar samples when ITBL added, the excitonic transition energy decreases by 12 meV for Ga-polar samples. These data support and confirm the above conclusion drawn from Raman scattering (Fig. 3).

Figs. 4 and 5 illustrate the results of positron annihilation. Fig. 4 reveals the S parameter as a function of the positron incident energy E. The incident positron energy E (keV) corresponds to an implantation profile in

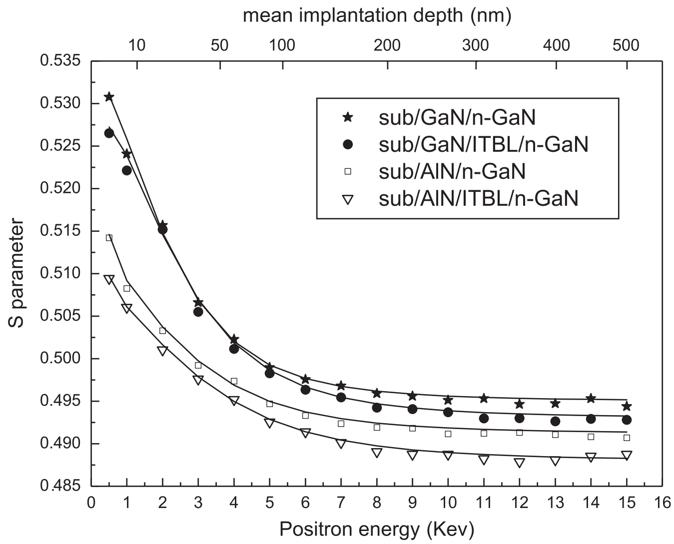

Fig. 4. S parameter versus positron energy for various samples, solid lines are the fitted curves. Mean penetration depth is indicated by the top axis.

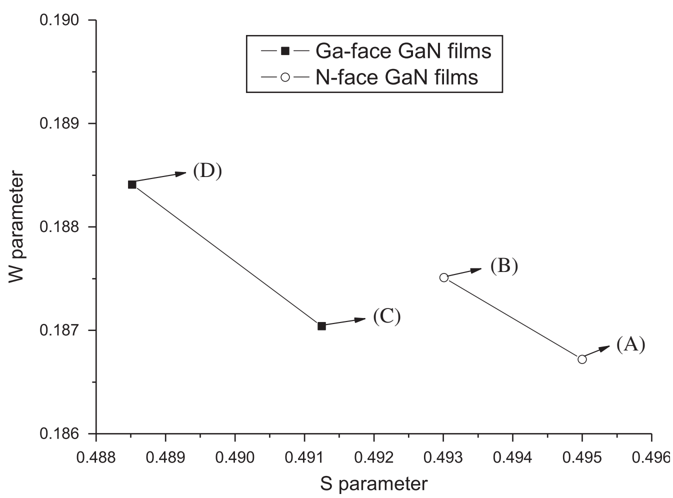

Fig. 5. The electron-momentum parameters S and W in various GaN samples.

materials [18],

$$P(z) = \frac{mz^{m-1}}{z_0^m} \exp[-(z/z_0)^m], \tag{2}$$

where $m = 2.0$, z_0 is given by

$$z_0 = \frac{\bar{z}}{\Gamma[(1/m) + 1]}, \tag{3}$$

$\bar{z}$ is mean stopping depth. The dependence of mean depth on energy is a power law,

$$\bar{z} = \frac{A}{\rho} E^n, \tag{4}$$

in Eq. (4) $A = 4.0\,\mu\mathrm{g\,cm^{-3}\,keV^{-1.6}}$, where ρ is target density ($\mathrm{g/cm^3}$), $n = 1.6$, $\bar{z}$ is in Å and E is in keV. After its introduction into solid, the energetic positron rapidly loses energy in the interaction with matter. Thereafter the positron lives a thermal equilibrium with environment, and its state develops in real space as a diffusion process. The thermalization and diffusion processes can be described as one-dimension diffusion equation:

$$D_+ n''(z) - (1/\tau_{\mathrm{eff}})n(z) + P(z) = 0, \tag{5}$$

where D_+ is diffusion coefficient of positrons, $n(z)$ is probability density of positrons at a distance z from the surface, $1/\tau_{\mathrm{eff}}$ is effective trapping rate, and $P(z)$ is implantation profile of positrons.

$$1/\tau_{\mathrm{eff}} = 1/\tau_{\mathrm{b}} + \kappa(z) = 1/\tau_{\mathrm{b}} + \mu C_{\mathrm{d}}, \tag{6}$$

where $1/\tau_{\mathrm{b}}$ is bulk annihilation rate, $\kappa(z) = \mu C_{\mathrm{d}}$, $\kappa(z)$ is trapping coefficient around the defect, C_{d} is defect concentration, and μ is a proportional factor. Diffusion length of positrons is given by

$$L_{\mathrm{eff}}(z) = \sqrt{D_+/(1/\tau_{\mathrm{b}} + \mu C_{\mathrm{d}})}. \tag{7}$$

Vepfit is the software package making use of physics model as described above [19]. We employ one layer model of the model 5 to fit data. The fitted results of S parameter and effective diffusion length L_{eff} are listed in Table 1.

3.1. Identification of vacancy

From Table 1, it can be seen that the effective diffusion lengths of all samples are no more than 46 nm. However, the typical value of effective diffusion length L_{eff} in semiconductors such as Si, Ge, GaAs, is 200–300 nm, and that in metals such as Ni and Cu, is 150–200 nm, it is obvious that L_{eff} in GaN samples are much shorter than the typical value of L_{eff} in defect-free materials, which reveals that positrons are trapped or scattered by open volume defects. According to Uedono and collaborators [20], undoped GaN (lateral epitaxial overgrowth), Si-doped GaN, Mg-doped GaN and undoped Ga-polar GaN have the same defect Ga vacancy V_{Ga}, and vacancy clusters or complexes appear in N-polar GaN.

The number of different vacancy-type defects trapping positron in materials can be investigated through the linearity between annihilation parameters S and W [21]. If only a single type of vacancy is present, W parameter depends linearly on S parameter when a fraction of positron annihilations varies. From the S–W plot, it clearly exhibits that two types defects appear in Ga-polar and N-polar GaN, respectively. Theoretically the formation energies of charged defects in thermal equilibrium are shown in Ref. [22], Ga vacancy (V_{Ga}) and $V_{Ga}{-}O$ complex have their lower formation energy than that of N vacancy (V_N), O_N and Si_{Ga} in n-type material. Saarinen and coworkers [21] have observed V_{Ga} and its complex in both bulk crystal and epilayer GaN in positron annihilation experiments. In addition, the results of Rummukainen et al. [23] showed that V_{Ga} and Ga vacancy clusters are present in Ga-polar and N-polar GaN films, respectively. Combined with the experimental and theoretical conclusion mentioned above, it is surmised that vacancies Ga exist in Ga-polar GaN films and the presence of Ga vacancy clusters is in the N-polar GaN films.

3.2. The effect of strain on defect

Different stress area has a distinct influence on solid chemical potential, chemical potential deviates $\sigma\Omega$ and $-\sigma\Omega$ from equilibrium individually in tensile and compressive environment. Here σ is residual stress in films, and Ω is vacancy volume. Vacancy formation energy decreases by $\sigma\Omega$ in tensile region, while in compressive area vacancy formation energy increases by $\sigma\Omega$, which means forming vacancy need more energy when compressive stress exists in the films, however, less energy could form vacancy in tensile stress region. Distinct residual stress could change the vacancy-type defect concentration in Ga-polar and N-polar GaN films. The relation between defect concentration and stress can be expressed as Ref. [24]:

$$C_{\mathrm{v}}^{\pm} = C\exp[(-\Delta G_{\mathrm{f}} \pm \sigma\Omega)/kT], \tag{8}$$

where $C_{\mathrm{v}}^{\pm}$ is vacancy amount in unit volume, '+' and '−' correspond to tensile and compress stress, respectively, C is atom number in unit volume, ΔG_{f} is vacancy formation energy, K is Boltzmann constant and T is Kelvin temperature. The results of Raman scattering show that tensile and compressive stress occur in N-polar and Ga-polar samples, respectively. Tensile stress makes vacancy formation energy diminishing. Therefore, V_{Ga} clusters can readily come into being in tensile area, there are higher defect concentration in N-polar samples; on the other hand, vacancy formation energy rises in compressive environment, thus less V_{Ga}s are present on account of larger formation energy, leading to lower defect concentration.

3.3. The improvement of ITBL on materials

From the results of Raman scattering, when Ga-polar and N-polar GaN films were added the ITBL layer individually, residual stress varies from 0.323 GPa to nearly 0 Gpa in Ga-polar samples. However, residual stress is not easy to be reduced in N-polar samples. It can be seen ITBL could effectively reduce stress in Ga-polar GaN films in contrast to N-polar GaN films. The information about slow positron annihilation reveals: the S parameter decreases by 0.0028 in Ga-polar sample with ITBL compared with Ga-polar sample without ITBL, while the effective diffusion length L_{eff} increases by 9 nm; appending the ITBL layer in N-polar sample, the S parameter diminishes 0.002, meanwhile L_{eff} grows up 5.4 nm. Since the epilayer is as thick as 1.8 μm, positron mean implantation depth is nearly 500 nm in the light of its maximum incident energy, so positron annihilation only brings out the information about epilayer defect.

Usually dislocation is introduced during the course of strain relaxation, dislocation lines mainly congregate at nearby the interface 300 nm range between buffer layer and substrate by scanning electron microscope (SEM) [12]. Some dislocation lines extend along c axis, they interact each other and some dislocation lines terminate others in buffer layer. As buffer layer thickness growing up, less and less dislocation lines could survive in the epilayer, which causes the dislocation defect going down. But the binding energy of positrons to the dislocations, so-called shallow traps, is relatively small, therefore these traps are important only at low temperature [25]. However, this experiment is performed at room temperature, we neglect the traps of positrons located dislocations. In Pi et al. paper [26], they have reported that Ga vacancies appear to prefer to reside alongside dislocations. The implementation of ITBL could induce stress relaxation to some extent, and prevents dislocations stretching to the surface, with dislocations reduction at the top layer V_{Ga} and Ga vacancy clusters lessen, leading to S parameter dropping and L_{eff} rising. So by implementing ITBL, vacancy size and concentration could be reduced in Ga-polar and N-polar materials to some extent.

Hall mobility also exhibits ITBL has a significant improvement on GaN films quality. From Table 1, it shows that carrier mobility increases by almost 5 and 1.5 times for N-polar and Ga-polar films with ITBL in contrast to the films with no ITBL, respectively. In accordance with Ng [27] and Lu [28] viewpoint, acceptor centers are introduced along dislocation line, which could act as the electron trappers. Electrons are scattered by dislocation line with negative charges, reducing electron mobility. So the carrier mobility increase means the decrease of electron trap and scattering center such as: dislocation lines, acceptor centers like V_{Ga} or Ga vacancy clusters.

4. Summary

In this work, Raman scattering, PL and slow-positron annihilation were used to observe the stress and defects in Ga-polar and N-polar GaN films, moreover stress relaxation and generation defects with ITBL for both polar GaN samples. The results of Raman scattering and PL spectra show: tensile stress is present in N-polar GaN samples while compressive stress is found in Ga-polar GaN samples, and ITBL could effectively relax stress in Ga-polar films in contrast to N-polar films. The outcomes of positron annihilation indicate that perhaps Ga vacancies are dominant defects in Ga-polar GaN samples and its clusters prevail in N-polar GaN samples. The residual stress has an effect on vacancy formation to some degree: Ga vacancies could be suppressed in compressive area, and Ga vacancy clusters are promoted in tensile area. When ITBL was added in two group samples, Ga vacancies and its clusters can be reduced through lessening the dislocation lines on the top layers.

Acknowledgment

This work was supported by the National Natural Science Foundation of China under no.10425072.

References

[1] S. Ruvimov, in: M.O. Manasreh (Ed.), Nitride Semiconductors: Electrical, Structural and Defects Properties, Elsevier, Amsterdam, 2000, p. 51.

[2] B.H. Leung, W.K. Fong, C. Surya, Appl. Surf. Sci. 212–213 (2003) 897.

[3] C.F. Zhu, W.K. Fong, B.H. Leving, C. Surya, Appl. Phys. A 72 (2001) 495.

[4] J.N. Kuznia, M.A. Khan, D.T. Olson, R. Kaplan, J. Freitas, J. Appl. Phys. 73 (1993) 4700.

[5] I. Akasaki, H. Amano, K. Hiramatsu, N. Sawaki, J. Crystal Growth 98 (1989) 209.

[6] C.H. Lee, G.C. Chi, C.F. Lin, M.S. Feng, J.D. Guo, Appl. Phys. Lett. 68 (1996) 3440.

[7] W.K. Fong, C.F. Zhu, B.H. Leung, C. Surya, J. Crystal Growth 233 (2001) 431.

[8] C. Kisielowski, J. Krüger, S. Ruvimov, T. Suski, J.W. Age, E. Jones, Z. Liliental-Weber, M. Rubin, E.R. Weber, M.D. Bremser, R.F. Davis, Phys. Rev. B 54 (17) (1996) 745.

[9] P. Perlin, C. Jauberthie-Carillon, J.P. Itie, A.S. Miguel, I. Grzegroy, A. Polian, Phys. Rev. B 45 (1992) 83.

[10] W. Brandt, A. Dupasquicr (Eds.), Positron Solid State Physics, North-Holland, Amsterdam, 1983.

[11] K. Sararinen, P. Hautojärvr, C. Corbel, in: M. Stavola (Ed.), Seminiconductors and Semimetals, vol. 51A, Academic, New York, 1998, p. 209.

[12] J. Xie, Master Thesis, University of Science and Technology of China, 2002.

[13] R. Han, X. Guo, H. Weng, Acta Phys. Sinica 37 (1988) 1517 (in Chinese).

[14] T. Kozawa, T. Kachi, H. Nagase, N. Koide, K. Nanabe, J. Appl. Phys. 77 (1995) 4389.

[15] B. Gil, O. Briot, R.-L. Aulombard, Phys. Rev. B 52 (1995) 17028.

[16] A. Shikanai, T. Azuhata, T. Sota, S. Chichibu, A. Kuramata, K. Horino, S. Nakamura, J. Appl. Phys. 81 (1997) 417.

[17] C. Kisielowski, J. Kruger, S. Ruvimov, T. Suski, J.W. Ager, E. Jones, Z. Liliental-Weber, M. Rubin, E.R. Weber, M.D. Bremser, R.F. Davis, Phys. Rev. B 54 (1996) 17745.

[18] P.J. Schultz, K.G. Lynn, Rev. Mod. Phys. 60 (1988) 701.

[19] A. Van Veen, H. Schut, J. de Vires, R.A. Hakvoort, M.R. Ijpma, in: P.J. Schultz, G.R. Massoumi, P.J. Simpson (Eds.), Slow Positron Beams for Solids and Surfaces, American Institute of Physics, New York, 1990, p. 171.

[20] A. Uedono, S.F. Chichibu, Z.Q. Chen, M. Sumiya, R. Suzuki, T. Ohdaira, T. Mikado, T. Mukai, S. Nakamura, J. Appl. Phys. 90 (2001) 181.

[21] K. Saarinen, in: M.O. Manasreh (Ed.), III–V Nitride Semiconductors: Electrical, Structural and Defects Properties, Elsevier, Amsterdam, 2000, p. 109.

[22] T. Mattila, R.M. Nieminen, Phys. Rev. B 55 (1997) 9571.

[23] M. Rummukainen, J. Oila, A. Laakso, K. Saarinen, A.J. Ptak, T.H. Myers, Appl. Phys. Lett. 84 (2004) 4887.

[24] K.-N. Tu, J.W. Mayer, L.C. Feldman, Electronic Thin Films Science, X. Huang, J. Du, K. Chen, Trans., Science Press, 1997.

[25] M.J. Puska, R.M. Nieminen, Rev. Mod. Phys. 66 (1994) 841.

[26] X.D. Pi, P.G. Coleman, C.L. Tseng, C.P. Buruows, B. Yavich, W.N. Wang, J. Phys.: Condens. Matter 14 (2002) L243.

[27] H.M. Ng, D. Doppalapudi, T.D. Moustakas, N.G. Weimann, L.F. Eastman, Appl. Phys. Lett. 73 (1998) 821.

[28] L.W. Lu, W.K. Fong, C.F. Zhu, B.H. Leung, C. Surya, J. Wang, W. Ge, J. Crystal Growth 234 (2002) 99.